Emulsion-Liquid-Membrane Extraction of Copper Using a Hollow-Fiber Contactor

Shih-Yao B. Hu and John M. Wiencek
Dept. of Chemical and Biochemical Engineering, The University of Iowa, Iowa City, IA 52242

A novel extraction technique using an emulsion liquid membrane within a hollow-fiber contactor was developed and utilized to extract copper using LIX 84 extractant. Emulsion liquid membranes are capable of extracting metals from dilute waste streams to levels much below those possible by equilibrium-limited solvent extraction. Utilizing an emulsion liquid membrane within a hollow-fiber contactor retains the advantages of emulsion-liquid-membrane extraction, namely, simultaneous extraction and stripping, while eliminating problems encountered in dispersive contacting methods, such as swelling and leakage of the liquid membrane. Mathematical models for extraction in hollow-fiber contactors were developed. The models satisfactorily predict the outcome of both simple solvent extraction and emulsion-liquid-membrane extraction of copper by LIX 84 in a hollow-fiber contactor over a wide range of conditions. Emulsion-liquid-membrane extraction performs exceptionally well when the extraction is close to equilibrium limit. It is also capable of extracting a solute from very dilute solutions. Stability of the liquid membrane is not crucial when used in hollow-fiber contactors; the surfactant in liquid membrane can be reduced or even eliminated without severely impairing the performance.

Introduction

Aqueous streams contaminated with heavy metal ions may be produced as effluents from industrial plants or during attempts to remediate solids loaded with heavy metals, such as contaminated soils. Although a number of processes exist for the treatment of aqueous streams containing heavy metals, one of the most promising techniques is solvent extraction using liquid ion exchange. Unlike precipitation methods (Peters and Ku, 1985), solvent extraction does not generate secondary waste that needs to be disposed in a landfill. Unlike electrochemical methods, solvent extraction is effective even with dilute feed streams. Metal solvent extraction has been extensively used in hydrometallurgical operations. More recently, dispersion-free solvent extraction using microporous hollow-fiber contactors has received considerable attention and was proven to be very effective (Alexander and Callahan, 1987; Yoshizuka et al., 1986; Matsumoto et al., 1987; Sato et al., 1989a,b, 1990; Goto et al., 1992, 1994; and Yun et al., 1993). Proficiency of solvent extraction, however, is limited by the extraction equilibrium.

Correspondence concerning this article should be addressed to J. M. Wiencek.

An emulsion liquid membrane (ELM) is an extraction system that can accomplish both extraction and stripping in one step. First invented by Li (1968), ELMs are made by forming an emulsion between two immiscible phases. Usually stabilized by surfactants, the water-in-oil emulsion contains the extracting agent in the oil phase and the stripping reagent in the aqueous receiving phase. This emulsion is then dispersed by mechanical agitation into a feed phase containing the metal to be extracted. Figure 1 shows an example of ELM extraction of copper(II) using an oxime extractant (RH), which follows a stoichiometry of one copper ion to two oxime molecules:

$$Cu^{2+} + 2RH \leftrightarrow CuR_2 + 2H^+ \qquad (1)$$

Combining the extraction and stripping processes can remove equilibrium limitations and reduce metal concentration in the feed to very low levels. Various liquid membrane formulations have been used to extract heavy metals such as copper, zinc, cadmium, nickel, mercury, lead, and chromium (Gu et

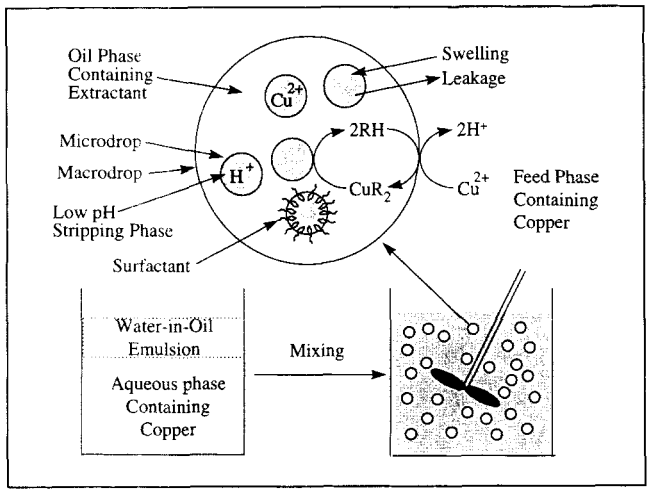

Figure 1. Copper extraction with an ELM.

By dispersing a water-in-oil emulsion into an aqueous feed phase, macrodroplets of emulsion are formed in the continuous aqueous phase. Copper(II) is transported to the emulsion-feed-phase interface and reacts with the complexing agent (RH) to form an oil-soluble copper complex (CuR_2). This complex diffuses to the interior of the emulsion droplet until it encounters a microdroplet of the internal phase where the metal ion is exchanged for hydrogen ion and the complexing agent is regenerated. The dispersion is then allowed to settle, and the lower aqueous stream is withdrawn for discharge. The upper emulsion is then demulsified to split the membrane and the enriched stripping phases.

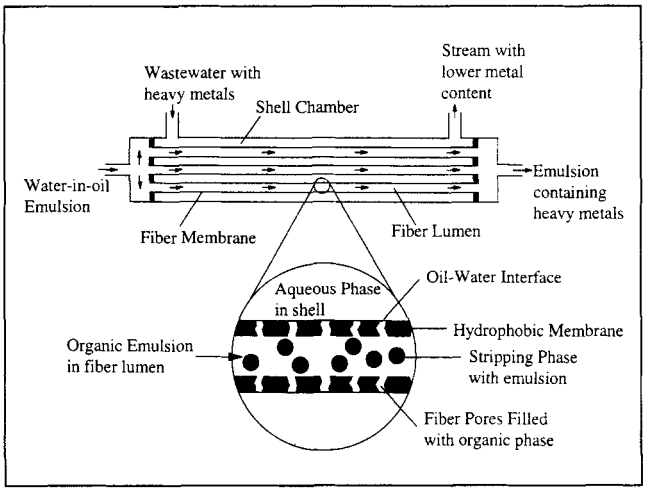

Figure 2. Emulsion-liquid-membrane extraction in a hollow-fiber contactor.

Interface is maintained at the pore mouth on the fiber outer surface by keeping the aqueous-feed phase pressure higher than that of the emulsion phase. Copper(II) is extracted into the organic phase of the emulsion by complexing with the carrier (LIX84). The internal droplets containing the stripping agent (sulfuric acid) strip the complex to trap copper as cupric sulfate.

al., 1986; Fuller and Li, 1984; Weiss and Grigoriev, 1982; Boyadzhiev and Bezenshek, 1983; Kitagawa et al., 1977; and Izatt et al., 1987). Demulsification (emulsion breaking) by application of high-voltage electric fields has proven to be a most successful technique for recovering the concentrated extract phase (Draxler et al., 1988). Heavy metals concentrated in the receiving phase can be recovered as a valuable product by electroplating or crystallization (as a single pure salt). The remaining oil phase can be recycled.

The ELM extraction in a stirred contactor as previously described has two main disadvantages (Raghuraman and Wiencek, 1993): (1) on prolonged contact with the feed stream, the emulsion swells with water, increasing the internal-phase volume. Swelling and water uptake cause a reduction in the stripping reagent concentration in the internal phase, which in turn reduces the stripping efficiency. Furthermore, the solute that has been concentrated in the internal phase is also diluted, resulting in lower separation efficiency of the liquid membrane. (2) Leakage of the internal-phase contents into the feed stream because of membrane rupture. Leakage, like swelling, also reduces the efficiency of separation. The leakage can be minimized by making more stable emulsions with optimized surfactant, but this makes the subsequent demulsification and product recovery steps more difficult. Lower shear rates would also minimize leakage, but mass-transfer resistances could then become very significant.

An ELM can be used to simultaneously extract and strip the metal from the wastewater by a liquid–liquid dispersion-free contacting in a hollow-fiber contactor (HFC) (Raghuraman and Wiencek, 1993). This arrangement combines the advantages of ELM separation (simultaneous extraction and stripping) and dispersion-free solvent extraction. The absence of high shear rates, which are encountered in agitated dispersion, minimizes leakage of the internal stripping phase. In addition, internal aqueous droplets cannot directly contact the feed aqueous phase, thus the possibility of swelling is greatly diminished. Figure 2 shows ELM extraction in a hydrophobic HFC.

This article presents mathematical models for ELM extraction as well as simple solvent extraction processes of copper in an HFC. Extraction efficiency of the two designs will be compared under various conditions. Besides previous work by our group (Raghuraman and Wiencek, 1993), a literature search revealed only two previous references in this area (a Dutch patent and a conceptual proposal by Cahn and Li (1988)). A somewhat similar design was investigated by Walsh and Monbouquette (1993). In their work, engineered metal-sorbing surfactant vesicles circulate through the tube side of a hollow-fiber cartridge, while metal bearing solution circulates on the shell-side. A lipophilic metal carrier in the phosphatidylcholine vesicle wall shuttles heavy metal ions to the aqueous vesicle core where an encapsulated water-soluble chelating agent complexes the ions, thereby providing the driving force for metal-ion sorption.

Theory

Figure 3 shows the transport model for this system. Aqueous solution containing copper ions flows through the shell side of the HFC while the organic phase flows through the tube (lumen) side concurrently. The chelating reaction occurs on the outer surface of the membrane. For ELM systems, equilibrium is assumed to be established instantaneously between the organic phase and internal phase because the vast contacting area provided by numerous internal droplets greatly accelerates the stripping reaction.

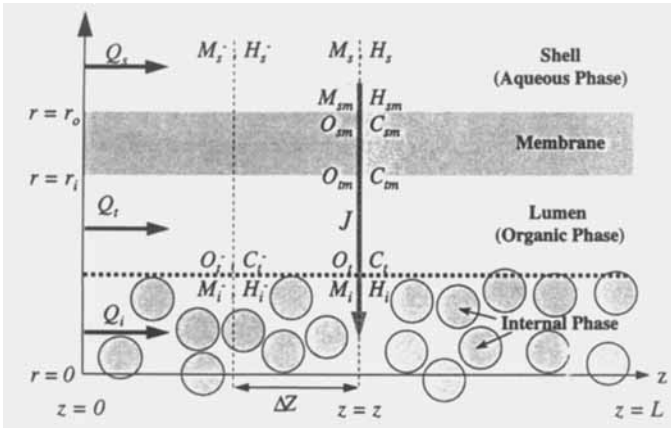

Figure 3. Modeling copper extraction in an HFC.

An aqueous feed phase containing copper flows through the shell side of HFC module while an emulsion flows through the tube side concurrently. The length of the HFC is divided into finite intervals and mass transfer in each interval is characterized by governing equations. Refer to the Notation section for symbol definitions.

Simple solvent extraction

The extraction process can be considered as four (or five when ELM is used) sequential steps that can be described mathematically within a differential cell Δz:

1a. Transport of copper ion on the shell side:

$$J_M^s = n\pi d_o \Delta z \cdot k_M^s (M_s - M_{sm}), \tag{2}$$

and the mass balance gives

$$J_M^s = Q_s (M_s^- - M_s). \tag{3}$$

1b. The counter transport of hydrogen ions on the shell side is also considered:

$$J_H^s = n\pi d_o \Delta z \cdot k_H^s (H_s - H_{sm}) \tag{4}$$

and

$$J_H^s = Q_s (H_s^- - H_s). \tag{5}$$

2. The chelating reaction on the membrane surface:

$$J_R = n\pi d_o \Delta z \cdot k_f \left(\frac{M_{sm} O_{sm}}{H_{sm}} - \frac{C_{sm} H_{sm}}{K_{eq} O_{sm}} \right). \tag{6}$$

3a. Diffusion of complex across the membrane:

$$J_C^m = n\pi d_{lm} \Delta z \cdot k_C^m (C_{sm} - C_{tm}). \tag{7}$$

3b. Diffusion of LIX across the membrane:

$$J_O^m = n\pi d_{lm} \Delta z \cdot k_O^m (O_{sm} - O_{tm}). \tag{8}$$

4a. Transport of the complex in the tube side:

$$J_C^t = n\pi d_i \Delta z \cdot k_C^t (C_{tm} - C_t) \tag{9}$$

and

$$J_C^t = Q_t (C_t - C_t^-) \tag{10}$$

4b. Transport of LIX in the tube side:

$$J_O^t = n\pi d_i \Delta z \cdot k_O^t (O_{tm} - O_t) \tag{11}$$

and

$$J_O^t = Q_t (O_t - O_t^-). \tag{12}$$

At steady state, all of these individual mass-transfer rates are equal to the overall mass-transfer rate J:

$$J = J_M^s = -\tfrac{1}{2} J_H^s = J_R = J_C^m = -\tfrac{1}{2} J_O^m = J_C^t = -\tfrac{1}{2} J_O^t. \tag{13}$$

Overall, there are 11 equations (Eqs. 2–12) to solve 11 unknowns (J, M_s, H_s, M_{sm}, H_{sm}, C_{sm}, O_{sm}, C_{tm}, O_{tm}, C_t, and O_t). One of the equations (Eq. 6) is nonlinear.

ELM extraction

When ELM is used, mass-balance equations (Eqs. 10 and 12) should be replaced by

$$J_C^t + J_M^i = Q_t (C_t - C_t^-) + Q_i (M_i - M_i^-) \tag{14}$$

and

$$J_O^t + J_H^i = Q_t (O_t - O_t^-) + Q_i (H_i - H_i^-). \tag{15}$$

In addition, there is a mass-balance equation for the internal phase

$$2 \cdot (M_i - M_i^-) = (H_i^- - H_i) \tag{16}$$

and the equilibrium between the bulk organic phase and the internal phase gives

$$K_{eq} = \frac{C_t \cdot H_i^2}{M_i \cdot O_t^2}. \tag{17}$$

Equation 13 becomes

$$J = J_M^s = -\tfrac{1}{2} J_H^s = J_R = J_C^m = -\tfrac{1}{2} J_O^m = J_C^t + J_M^i = -\tfrac{1}{2} (J_O^t + J_H^i). \tag{18}$$

In this system, there are 13 equations (Eqs. 2 to 8, 9, 11, and 14 to 17) to solve 13 unknowns (J, M_s, H_s, M_{sm}, H_{sm}, C_{sm}, O_{sm}, C_{tm}, O_{tm}, C_t, O_t, M_i, and H_i). Two of the equations (Eqs. 6 and 17) are nonlinear.

Modeling algorithm

Each case results in a set of nonlinear equations that must be solved simultaneously. Broyden's multidimensional secant methods discussed in *Numerical Recipes* (Press et al., 1992) was implemented to solve the problem numerically. Subroutine broyden.f and its related subroutines were used with minor modification in our FORTRAN programs. The algorithm for solving the problem is:

1. M_s, H_s, C_t, O_tM_i, H_i at the inlet ($z = 0$) of the HFC are experimentally fixed. These are the current M_s^-, H_s^-, C_t^-, $O_t^-M_i^-$, H_i^-.
2. The equations are solved simultaneously to get all concentrations at $z = z + \Delta z$, including M_s, H_s, C_t, O_t, M_i, H_i.
3. All the superscript "$-$" terms are replaced with the newly calculated values. The process is repeated until $z \geq L$.

Experimental Methods

The source for copper was copper(II) sulfate pentahydrate (Certified ACS grade, Fisher Scientific). LIX84 was supplied as approximately 48 wt. % in kerosene by Henkel Corporation and was used without further purification. The chemical structure of LIX84 appears below:

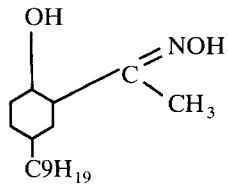

Solvent tetradecane (99%, technical grade), was purchased from Humphrey Chemicals. Surfactant ECA 5025 (currently marketed commercially as Paranox 106), a petroleum-based mixture of amine surfactant was donated by Exxon Chemical Company. Sulfuric acid (trace-metal grade) was purchased from Fisher Scientific. The HFC used was an Enka LM-2P06. The specifications for this membrane can be found in Table 1. Unless otherwise noted, all the emulsions used in the study consisted of 80 v/v % organic phase and 20 v/v % 6 N H_2SO_4. The organic phase consisted of 1 wt. % ECA 5025 as surfactant and variable amounts of LIX84 and tetradecane. Emulsions were prepared by mixing the organic phase and the aqueous phase in a Fisher Scientific ultrasonic dismembrator. Viscosity was measured with two Fisherbrand calibrated Ubbelohde viscometers (size 1 for 2 to 10 cSt and size 0 C for 0.6 to 3 cSt). Copper concentration in ppm level was analyzed on a Perkin-Elmer Plasma 400 ICP spectrophotometer; concentration in ppb level was analyzed on a Perkin-Elmer 2730 Graphite Furnace Atomic Absorption Spectrophotometer. Organic-phase copper content was determined by back extracting organic solution with 6 N H_2SO_4, then analyzing the resulting aqueous solution. All of the standards and samples were prepared or diluted with 6 N H_2SO_4 to reduce matrix effects during ICP analysis. Emulsion breakage was accomplished by an electrostatic coalescence cell powered by a Hipotronics AC Dilectric Test Set Model 730-1. The configuration is similar to the one used by Larson et al. (1994). The demulsification cell was modified to utilize a 50-mL polypropylene centrifuge tube.

Table 1. Manufacturer's Specifications for Enka LM-2P06 Hollow-Fiber Contactor

Length	Shell ID	Fiber Number	Pore Size	Fiber OD	Fiber ID
24 cm	1.5 cm	85	0.2 μm	0.1 cm	0.06 cm

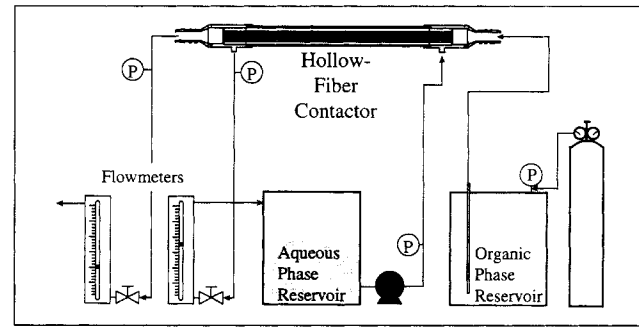

Figure 4. Typical experiment.

A hydrophobic membrane is used in this example; organic phase is delivered by a pressure vessel in once-through mode and flows through the tube side. Aqueous phase, delivered by a pump in total-recycle mode, flows through the shell side of the hollow-fiber module. To prevent the organic-phase from flowing out of the membrane pores and mixing with the aqueous phase, a higher pressure (about 5 psi difference) is applied to the aqueous side.

Figure 4 shows a typical experimental setup. In this case, organic phase was delivered by a pressure vessel (Fisherbrand) in once-through mode and flows through the tube side. Aqueous phase, delivered by a pump (Cole-Parmer Masterflex 7522-10) in total-recycle mode, flows through the shell side of the hollow-fiber module. To prevent the organic phase from flowing out of the membrane pores and mixing with the aqueous phase, a higher pressure [about 5-psi (34-kPa) difference] is applied to the aqueous side. When fluid is delivered by a pressure vessel, the pressure of the system is controlled by the pressure regulators connected to the pressure source (a cylinder of inert gas) and the flow rate is adjusted by the needle valve on the flowmeter at the outlet of the module. When the fluid is delivered by a peristaltic pump, the flow rate is controlled by the speed of the pump, while pressure is determined by the openness of the needle valve. The pressure vessel is more suitable for delivering low flow rates since the pulsation produced by the peristaltic pump is most significant at lower pump speeds and the mass transfer might be affected by such pulsation. The pump, on the other hand, has the advantage of being able to operate in a total recycle mode.

Results and Discussion

Parameters for modeling

The equilibrium constant ($K_{eq} = 3.897$) and mass-transfer correlations of the system have been obtained from separate studies (Hu, 1997). For the shell side, the mass-transfer correlation is

$$Sh = 0.245 \cdot Re^{0.6} Sc^{0.33}. \tag{19}$$

For the tube side,

$$Sh = 1.895 \cdot Pe^{0.33} \tag{20}$$

and for the membrane,

$$k_{mem} = 14.74 \cdot D \text{ cm/s}. \tag{21}$$

These correlations generally agree with comparable values reported in the literature (Prasad and Sirkar, 1988; Yang and Cussler, 1986; Wickramasinghe et al., 1992). Diffusivities of copper ion and hydrogen ion were calculated from the Nernst–Haskell correlation (Reid et al., 1987) as 7.4×10^{-6} and 2.2×10^{-5} cm^2/s at 70°F (21°C). These are estimates at infinite dilution. Since the copper solutions in this study are generally in the ppm level and no strong acid is added, these values are adopted without modification. The diffusivity of oxime in tetradecane at infinite dilution, calculated from the Hayduk and Minhas correlation (Reid et al., 1987), is 4.54×10^{-6} cm^2/s. This may not be a correct estimation because (1) the LIX84 concentration used in this study ranges from 1 wt. % to 10 wt. %, not at infinite dilution; and (2) the original LIX84 as shipped by Henkel contains 48 wt. % active ingredient (the oxime) dissolved in kerosene. After it is diluted in tetradecane, a multicomponent system is formed while the correlation is intended for binary systems. Nevertheless, the extraction process is likely to be controlled by the aqueous mass-transfer and/or chelating reaction. Errors in estimating diffusivities of organic species should not significantly affect the accuracy of the overall model. This assumption will be examined further in the later sections. The reaction rate constant k_f has been estimated to be approximately 1×10^{-6} cm/s (Hu, 1997), but the exact number is yet to be determined. This rate constant is the only adjustable parameter in the model. The diffusivities of oxime and the complex were assumed to be equal, which is common practice in facilitated transport modeling (Ho and Li, 1992). Viscosity of copper(II) solution was assumed to be identical to water, since the concentrations were only in the ppm level. Kinematic viscosity of LIX84 tetradecane solution varied little (0.028 Stoke at 2 wt. % to 0.030 Stoke at 10 wt. %) so the average of 0.029 Stoke was used. Viscosity of the emulsions was difficult to measure due to non-Newtonian behavior. The viscosity of emulsion is known to change due to shear stress, creaming of the droplets, and coalescence (Schramm, 1992). Measured viscosities of the solutions used in the study ranged from 0.042 to 0.053 Stoke with little reproducibility. Again, if the organic phase and the membrane contribute little resistance toward the extraction processes, the viscosities need not be exact. The average 0.048 Stoke was used.

Forward reaction rate constant

A total of 52 sets of data were sampled at various conditions in once-through simple solvent extraction. The reaction rate constant k_f was adjusted to minimize the objective function

$$\frac{1}{N}\sum^{N}(C_{exp}-C_{pred})^2/C_{exp}, \tag{22}$$

where C_{exp} is the aqueous copper concentration leaving the HFC obtained from experiments and C_{pred} is the concentrations predicted by the model at a certain k_f. N is the number of sets of data successfully solved by the program. The average ($1/N$) of the sum of least-square norm is implemented because at times the program fails to converge. For example, at one k_f, all of the 52 sets of experimental conditions converge in simulation ($N = 52$); at another k_f, 4 of the 52 conditions may fail to converge ($N = 48$). If the average was not taken, the sum of the least-square norm at the first k_f (which is the sum of 52 numbers) could easily be larger than that at the second k_f (which is a sum of only 48 numbers) even though the first k_f provides a better fit to the data. Divergence can happen because nonlinear systems of equations are in nature difficult to solve. The program works nearly flawlessly in simple solvent extraction, which has only one nonlinear equation (Eq. 6). For the ELM model, another nonlinear equation (Eq. 17) also needs to be solved simultaneously. There is currently no "perfect" numerical method to solve such problems (Press et al., 1992).

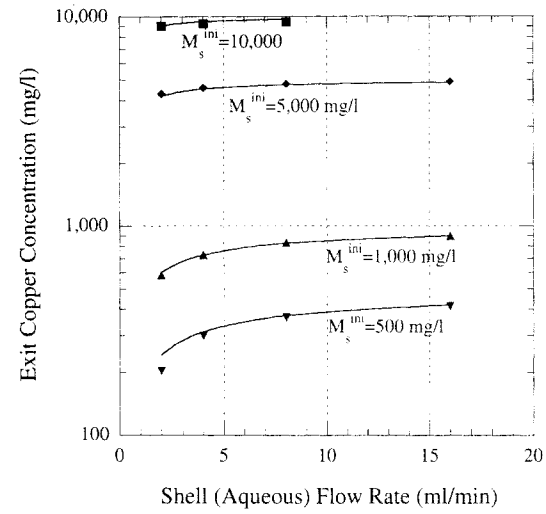

Figure 5. Modeling simple solvent extraction—effect of M_s^{ini} and Q_s.

Comparing experimental data (symbols) with model simulations (lines) of simple solvent extraction. Extractions at various aqueous-phase flow rates and initial copper concentrations are shown here. The organic-phase flow rate Q_t is 2 mL/min and the initial LIX concentration O_t^{ini} is 5 wt. % in all cases.

The constant (k_f) was regressed to be 9.28×10^{-6} cm/s. This value is very close to the 9.0×10^{-6} obtained by Yun et al. (1993), who used *n*-heptane as solvent. It is consistent with the value previously estimated (approximately 10^{-6} cm/s) by the authors (Hu, 1997).

Figures 5 to 7 show some representative results from both the experiments and the simulations. A single forward reaction rate constant 9.28×10^{-6} cm/s gives satisfactory prediction over a wide range of initial copper concentration, initial oxime concentration, and shell and tube flow rate. The average relative deviation calculated from Eq. 22 is only 2.8% for 52 data sets.

Relative resistances of the transport processes

Once the reaction rate constant was determined, the resistance of the extraction processes under various operating

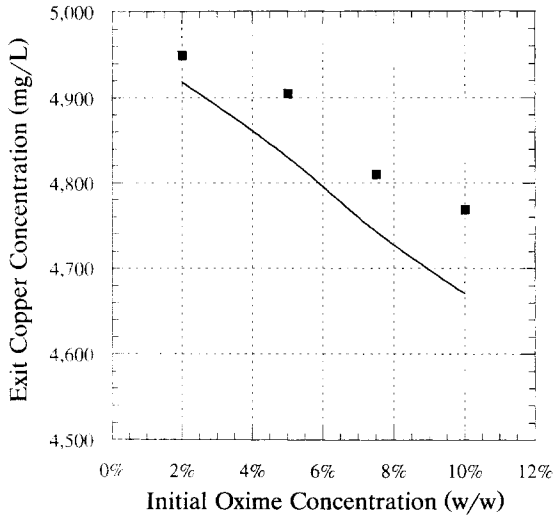

Figure 6. Modeling simple solvent extraction—effect of O_t^{ini}.

Comparing experimental data (symbols) with model simulations (lines) of simple solvent extraction. Extractions at various initial LIX84 concentration are shown here. The initial aqueous copper concentration M_s^{ini} is 5,000 mg/L, the aqueous-phase flow rate M_s is 4 mL/min, and the organic phase flow rate Q_t is 4 mL/min.

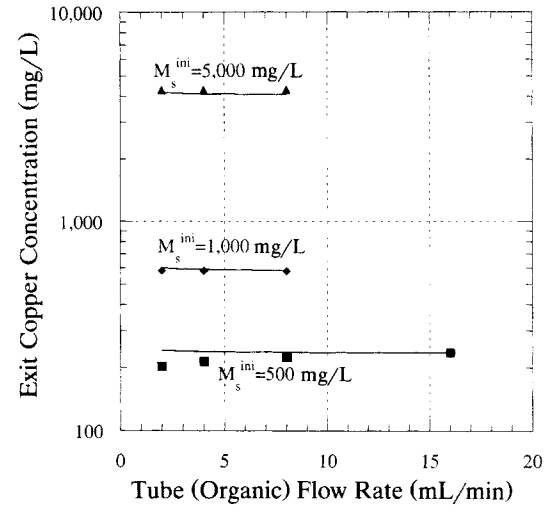

Figure 7. Modeling simple solvent extraction—effect of M_s^{ini} and Q_t^{ini}.

Comparing experimental data (symbols) with model simulations (lines) of simple solvent extraction. Extractions at various organic-phase flow rates and initial copper concentrations are shown here. The aqueous-phase flow rate Q_s is 2 mL/min and the initial LIX concentration O_t^{ini} is 5 wt. % in all cases.

conditions was examined. When Eqs. 2, 6, 7, 9, and 13 are combined, one obtains

$$J = A_s K\left(M_s - \frac{C_t}{K_p}\right), \tag{23}$$

where A_s is the surface area of the shell side of the membrane in a cell Δz and

$$\frac{1}{K} = \frac{1}{k_M^s} + \frac{1}{O_{sm}/H_{sm}\cdot k_f} + \frac{1}{A_{lm}/A_s\cdot K_p\cdot k_c^m} + \frac{1}{A_t/A_s\cdot K_p\cdot k_C^t}, \tag{24}$$

where A_{lm} and A_t are the log-mean membrane surface area and the tube-side membrane surface area, respectively. The pseudopartition coefficient K_p is defined as

$$K_p = \frac{K_{eq}O_{sm}^2}{H_{sm}^2}. \tag{25}$$

The four terms on the righthand side of Eq. 24 are the resistance contributed by shell-side mass transfer, reaction, membrane phase mass transfer, and organic phase mass transfer, respectively. O_{sm}/H_{sm} and K_p change along the axis, so the log-mean value was taken. The results from the model prediction are plotted in Figure 8.

In most cases, resistance from the chelating reaction controls the rate of the extraction process. The membrane-phase mass-transfer resistance is usually more than two orders of magnitude lower than the reaction resistance, and the organic-phase resistance is even smaller. Aqueous-phase mass transfer can be rate-controlling when the aqueous-phase flow rate is very low (Figure 8a), copper concentration is very low (Figure 8c) and oxime concentration is very high (Figure 8d). Unless it is extremely low or the extraction has approached the equilibrium limit, organic phase flow rate usually has no effect on the overall extraction (Figure 8b). To optimize the extraction process, a moderate flow rate in both phases is recommended for better mass transfer and reduced extractant loading requirements. Under such a "normal" condition, resistance from the reaction is higher than all other transport processes, even at low copper concentration (Figure 8e). This is also true in all of our simple solvent-extraction experiments in the HFC. It can also be observed that the membrane-phase resistance and the organic-phase resistance always move in the same direction as the reaction resistance, but remain at least an order of magnitude smaller. This is reasonable since the reaction term in Eq. 24 varies with O_{sm}/H_{sm}, while the membrane term and the organic term vary with K_p, which is proportional to $(O_{sm}/H_{sm})^2$. The results also suggest that diffusivity of the oxime and complex and the viscosity of the organic phase need not be estimated exactly because the mass-transfer rate of these two species has little, if any, impact on the overall extraction processes.

ELM extraction model

A total of 62 sets of data were collected for once-through ELM extraction in the HFC under various conditions. All of the emulsions used consisted of 80 v/v % organic phase and 20 v/v % 6 N sulfuric acid. When the same k_f value obtained from simple solvent extraction was used, however, the model usually underpredicted the exit copper concentration. Since the reaction is the main rate-controlling step, the rate constant was adjusted again to minimize the same object func-

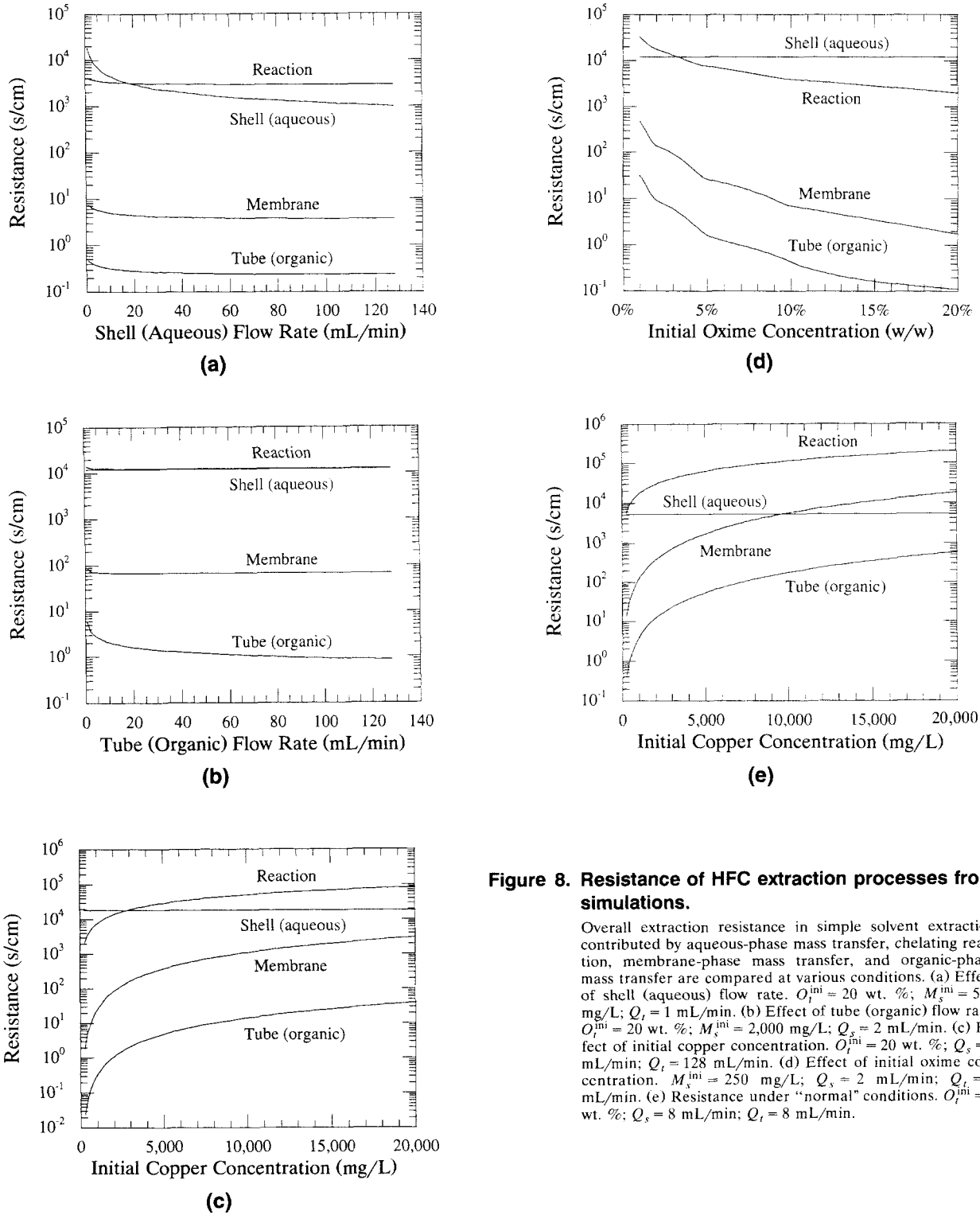

Figure 8. Resistance of HFC extraction processes from simulations.

Overall extraction resistance in simple solvent extraction contributed by aqueous-phase mass transfer, chelating reaction, membrane-phase mass transfer, and organic-phase mass transfer are compared at various conditions. (a) Effect of shell (aqueous) flow rate. $O_t^{ini} = 20$ wt. %; $M_s^{ini} = 500$ mg/L; $Q_t = 1$ mL/min. (b) Effect of tube (organic) flow rate. $O_t^{ini} = 20$ wt. %; $M_s^{ini} = 2{,}000$ mg/L; $Q_s = 2$ mL/min. (c) Effect of initial copper concentration. $O_t^{ini} = 20$ wt. %; $Q_s = 1$ mL/min; $Q_t = 128$ mL/min. (d) Effect of initial oxime concentration. $M_s^{ini} = 250$ mg/L; $Q_s = 2$ mL/min; $Q_t = 1$ mL/min. (e) Resistance under "normal" conditions. $O_t^{ini} = 5$ wt. %; $Q_s = 8$ mL/min; $Q_t = 8$ mL/min.

tion (Eq. 22). Aqueous-phase mass transfer may be slow at times but should not be affected by the use of ELM. It was found that reducing the reaction rate constant k_f from 9.28×10^{-6} cm/s to 2.32×10^{-6} cm/s gives the best fit to experimental data overall. The average relative deviation for this k_f is 3.6%.

Figure 9 shows some representative data from both the experiments and the simulations. It is obvious that $k_f = 2.32 \times 10^{-6}$ cm/s fits the experimental data better than the original k_f (9.28×10^{-6} cm/s). Potential explanations for the slower reaction kinetics in the ELM system are (1) some surfactant molecules absorb to the aqueous-emulsion interface and oc-

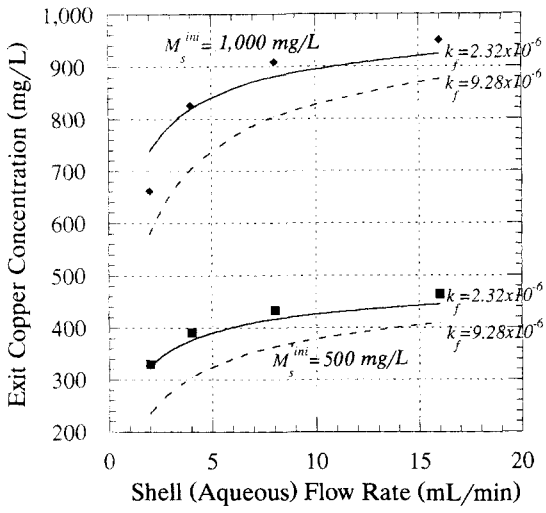

Figure 9. Adjusting k_f for ELM extraction modeling.

When the same k_f value regressed from simple solvent extraction was used directly for ELM extraction, the model (dashed lines) underpredicted the exit copper concentration (symbols). Since the reaction is the main rate-controlling step, the rate constant in the ELM extraction model was adjusted to fit the experimental data. It was found that reducing the reaction-rate constant k_f from 9.28×10^{-6} cm/s to 2.32×10^{-6} cm/s gives the best fit to experimental data overall (solid lines). The organic-phase flow rate Q_t is 4 mL/min and the initial LIX 84 concentration O_t^{ini} is 5 wt. % in all data.

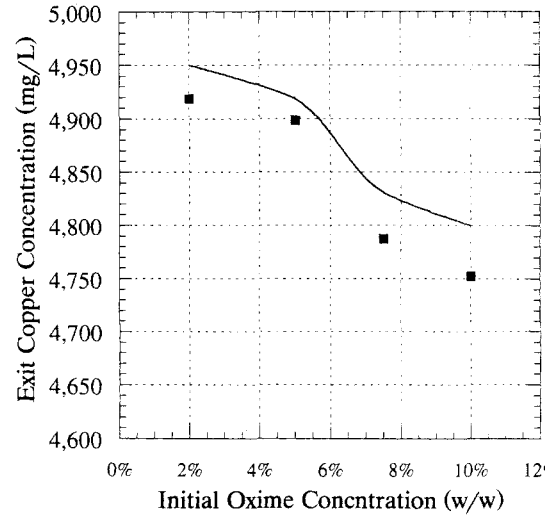

Figure 11. Modeling ELM extraction—effect of O_t^{ini}.

Comparing experimental data (symbols) with model simulations (line) of ELM extraction. Extractions at various initial LIX84 concentration O_t^{ini} are shown here. The initial copper concentration is 5,000 mg/L, the aqueous flow rate is 4 mL/min, and the organic-phase flow rate Q_t is 16 mL/min.

cupy available contacting area for the reaction (Wiencek and Qutubuddin, 1992), and (2) the surfactant interacts with the oxime physically or chemically and changes the reaction rate constant. More studies are required before a definitive conclusion can be reached. Meanwhile, after k_f is adjusted, the model gives excellent prediction over a wide range of conditions (Figures 10 to 12).

Comparing simple solvent extraction with ELM extraction in HFCs

The data from simple solvent extraction and ELM extraction were compared and some representative data are shown in Figure 13. The legend SS represents simple solvent extrac-

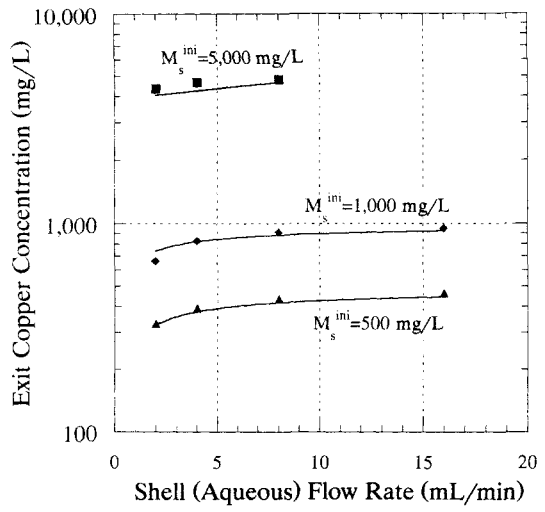

Figure 10. Modeling ELM extraction—effect of M_s^{ini} and Q_s.

Comparing experimental data (symbols) with model simulations (lines) of ELM extraction. Extractions at various aqueous-phase flow rates and initial copper concentrations are shown here. The organic-phase flow rate Q_t is 2 mL/min and the initial LIX concentration O_t^{ini} is 5 wt. % in all cases.

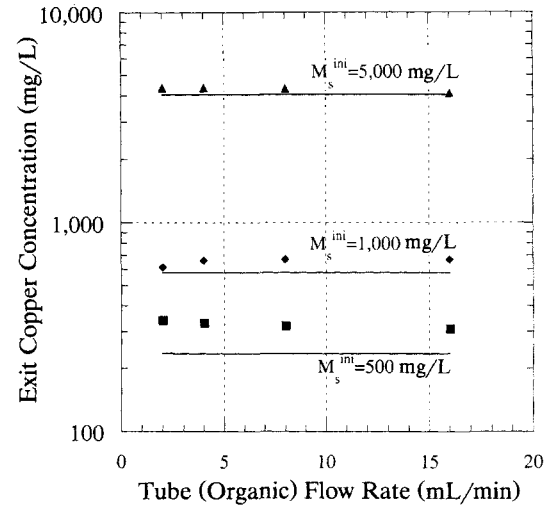

Figure 12. Modeling ELM extraction—effect of M_s^{ini} and Q_t.

Comparing experimental data (symbols) with model simulations (lines) of ELM extraction. Extractions at various organic-phase flow rates and initial copper concentrations are shown here. The aqueous-phase flow rate Q_t is 2 mL/min and the initial LIX concentration O_t^{ini} is 5 wt. % in all data.

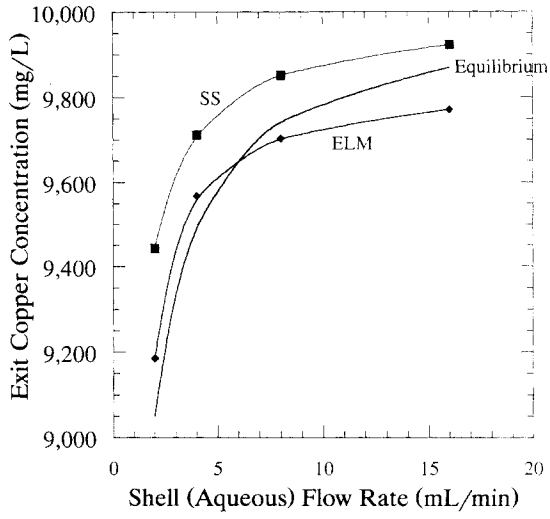

(a)

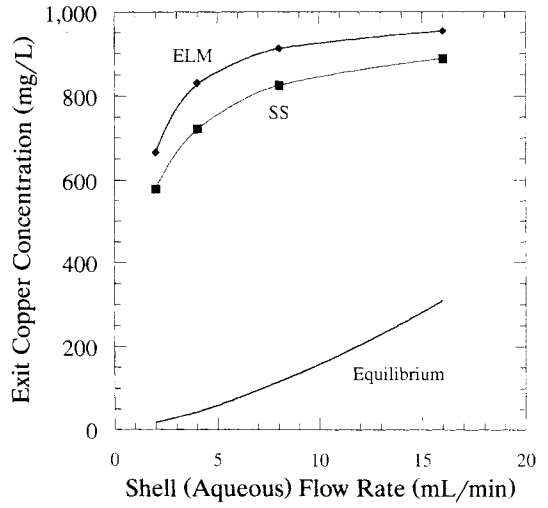

(b)

Figure 13. Comparing simple solvent extraction with ELM extraction in an HFC.

The data are from the experiments and the lines are smooth fits from the data (not from simulation). The legend SS represents simple solvent extraction, whereas ELM represents extraction using ELM. (a) When extraction approaches equilibrium, ELM extraction outperforms simple solvent extraction. The initial copper concentration M_s^{ini} is 10,000 mg/L, the initial LIX 84 concentration O_t^{ini} is 5 wt. %, and the organic-phase flow rate Q_t is 1 mL/min. (b) When extraction is far away from reaching equilibrium, simple solvent extraction has faster kinetics than ELM extraction. The initial copper concentration M_s^{ini} is 1,000 mg/L, the initial LIX 84 concentration O_t^{ini} is 5 wt. %, and the organic-phase flow rate Q_t is 8 mL/min.

tion, whereas ELM represents extraction using ELM. The points in the plots are taken from experimental data and the lines are from interpolations (i.e., not from model simulations). The comparisons are based on the same organic solution flow rate. For example, $Q_t = 4$ mL/min means data at a tube (organic phase) flow rate of 4 mL/min in simple solvent extraction are compared with data at a tube (emulsion) flow rate of 5 mL/min in ELM extraction because the emulsion

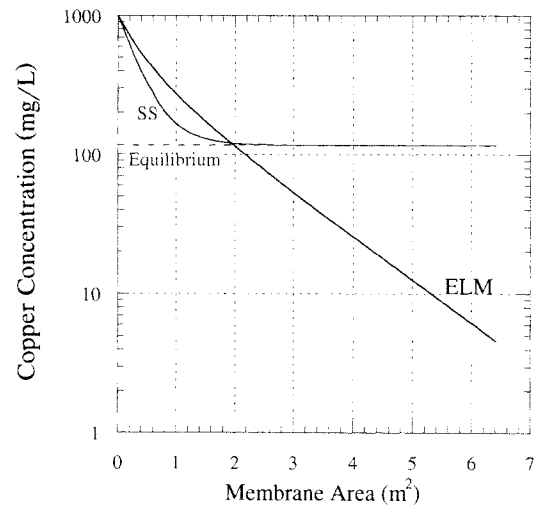

Figure 14. Extraction in an "imaginary" HFC.

To demonstrate the potential of ELM extraction in HFCs, simulations were conducted on an "imaginary" HFC module that is 100 times longer than the module used in this work. Aqueous and organic flow rate (Q_s and Q_t) were set at 4 mL/min, initial copper concentration M_s^{ini} was set at 1,000 mg/L, and 5 wt. % LIX84 was chosen as the extracting phase (O_t^{ini}). The resultant copper concentration is plotted vs. the axial length (presented as the membrane surface area). Simple solvent extraction (SS) shows faster initial rate but the slope decreases as it approaches equilibrium (the dash line in the figure). ELM shows slower initial rate, but the rate is consistent throughout. The aqueous copper concentration is reduced from 1,000 mg/L to about 4.5 mg/L, and the trend continues if the module is even longer.

consists of 20 v/v % aqueous phase and 80 v/v % organic phase.

It is not surprising that ELM extraction outperforms simple solvent extraction when the extraction is near the equilibrium limit, as shown in Figure 13a. This tends to happen when the aqueous phase is concentrated, aqueous flow rate is high, organic-phase flow rate is low, and oxime concentration is low. In this particular case, when simple solvent extraction extracted about 13% of the copper in aqueous phase, ELM extraction was able to achieve a 50% extraction by eliminating the equilibrium limitation. On the other hand, if the extraction is far from the equilibrium limit (Figure 13b), the faster kinetics of simple solvent extraction results in a higher level of extraction.

Because of the limited surface area of our lab-scale HFC (outer surface area of the membrane is only 638 cm^2), the level of extraction is generally low using once-through flow. To demonstrate the potential of ELM extraction in HFCs, simulations were conducted on an "imaginary" HFC module that is 100 times longer than the module used in this work. All other properties were assumed to remain the same and pressure drop along the length of the module was ignored. Aqueous and organic flow rate were assumed to be 4 mL/min, initial copper concentration was assumed to be 1,000 mg/L, and 5 wt. % LIX84 was chosen as the extracting phase. The results are shown in Figure 14 in which copper concentration is plotted vs. the axial length (presented as the membrane surface area). Simple solvent extraction shows faster initial rate, but the slope decreases as it approaches equilibrium (the dash line in the figure). Extraction roughly ceases at about

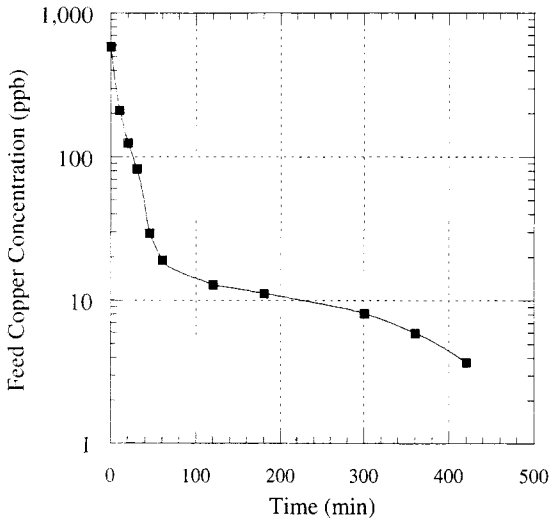

Figure 15. ELM extraction in an HFC–low feed concentration.

The ELM extraction was started with 580 ppb copper(II) in the aqueous phase using total recycle mode. The aqueous-phase volume is 500 mL and the organic-phase volume is 100 mL. The emulsion consists of 80 v/v % organic phase and 20 v/v % 6 N sulfuric acid. The organic phase contains 10 wt. % LIX 84, 1 wt. % ECA 5025, and 89 wt. % tetradecane. The symbols are from experimental measurements and the line is from interpolation of the data. The extraction took a long time because of the small contacting area of the module, but the feed concentration was reduced to less than 4 ppb.

116 mg/L. ELM shows slower initial rate, but the rate is consistent throughout. The aqueous copper concentration is reduced from 1,000 mg/L to about 4.5 mg/L and the trend continues if the module is even longer. ELM extraction starts to have an advantage over simple solvent extraction when this module approaches 2 m^2. Since a typical industrial-scale membrane device has a surface area ranging from 3 to 10 m^2, the potential industrial application of ELM extraction in HFCs is demonstrated by this simulation. The main consideration in scaling up this design is maintaining a pressure deference between the two phases because of higher pressure drop in larger devices. In the current case, the pressure drop in the tube side can be estimated based on the friction factor of flow in tubes (Bird et al., 1971):

$$f = \frac{1}{4}\left(\frac{d_i}{L}\right)\left(\frac{\Delta P}{\frac{1}{2}\rho u^2}\right) \tag{26}$$

where $f = 16/Re$ for laminar flow. In this case, tube flow rate is 5 mL/min, which translates into a Re of 0.433 inside each fiber lumen, and the pressure drop inside this 24-m-long, imaginary HFC would only be 4.38 psi (30.18 kPa), a demand well achievable by industrial instrumentation. The aqueous phase, having a lower viscosity, should not produce a significant pressure drop under laminar conditions either.

Another way to simulate an extremely long HFC module is to use total recycle mode instead of once-through mode. In total recycle mode, the fluids are delivered from the reservoirs through the HFC, then directed back to the reservoirs. The solution concentrations in the reservoirs are analyzed over time. The experiments discussed in the next two sections were conducted in total recycle mode. A mathematical model for total recycle mode has not yet been developed.

Extraction at low feed concentration

Some techniques for metal separation such as electrochemical methods are known to have low efficiency when dealing with dilute feed streams. In this particular experiment, the ELM extraction was started at an extremely low copper concentration (580 ppb). The extraction took a long time because of the small contacting area of the module, but the feed concentration was reduced to less than 4 ppb (Figure 15). This result suggests that ELM extraction is effective on very dilute feed streams.

Effect of surfactant concentration

Stability of ELM depends mostly on the surfactant concentration. When used in dispersive extractions such as in a stirred tank, the emulsion stability is crucial to successful extraction and leakage minimization. However, if the emulsion is too stable, it can make the downstream demulsification more difficult.

It has been shown that using ELM together with HFCs can minimize leakage and swelling (Raghuraman and Wiencek, 1993). The possibility of eliminating the use of surfactant was examined in this study. Figure 16 compares successful ELM extraction in an HFC with varying surfactant concentrations. Even with the case where no surfactant was used, there was no leakage of the stripping phase into the feed phase. Thus, emulsion stability is less relevant in an HFC/ELM extraction. On the other hand, the surfactant concentration does affect the extraction rate. It can be observed that during early

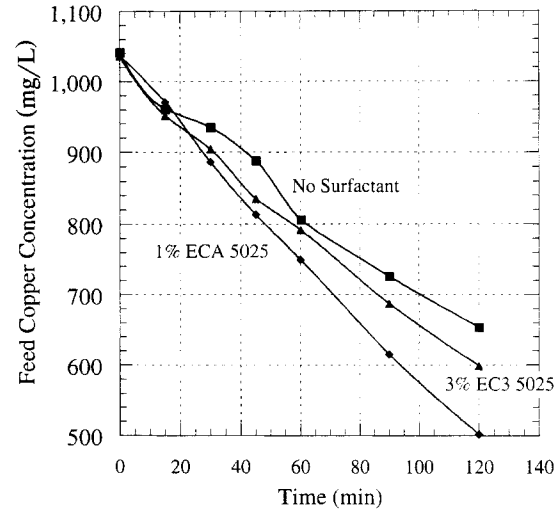

Figure 16. Effect of surfactant concentration.

Total recycle mode, ELM extraction in HFC using various surfactant concentrations are compared. The aqueous-phase volume is 600 mL and the emulsion volume is 120 mL. The content of the emulsion is the same as in Figure 15. The symbols are from experimental data and the lines are from interpolation of the data. The extraction performs well even without surfactant, suggesting the possibility of eliminating the downstream demulsification process.

stages of the extraction, comparable extracting rates were achieved by all three conditions. As the extraction proceeds, the highest rate was accomplished by using 1% surfactant, while the slowest rate was observed for the system using no surfactant. As discussed earlier, the initial extraction rate is controlled by the reaction resistance because the condition is far from equilibrium. In the later stages, however, the rate of extraction could be limited by the stripping rate. This stripping rate is further scaled to the area of the emulsion drops. The surfactant can increase this area by stabilizing smaller emulsion droplets. This would explain the higher extraction rate with 1% and 3% compared to 0% surfactant emulsions where higher areas are obtained if the stripping phase is dispersed as fine droplets in the oil phase (as in an emulsion) rather than just a physical mixture of the two phases. While 1% surfactant stabilizes the emulsion as well as 3% surfactant, the highest rates were obtained from 1% surfactant emulsion. This observation is consistent with previous results (surfactant molecules adsorb to the aqueous–organic interface and/or possibly interfere with the reaction mechanisms); higher surfactant concentrations tend to slow the extraction reaction at the membrane interface.

Conclusion

Copper extraction experiments in an HFC using simple solvent extraction and ELM were conducted. Predictive models for both extraction processes were successfully developed. Used as an adjustable parameter in the model, the forward reaction rate constant, regressed from experimental data, was determined to be 9.28×10^{-6} cm/s. A single rate constant gives excellent prediction over a wide range of conditions. For ELM extraction, it was found that the model can give satisfactory prediction over a wide range of conditions if the rate constant was reduced to 2.23×10^{-6} cm/s. ELM, though having slower extraction kinetics, shows exceptional extraction capacity when the extraction approaches or exceeds equilibrium. It eliminates equilibrium limitation of solvent extraction even at low oxime concentration. In total-recycle mode experiments, it was shown that the ELM can successfully extract metal even at very low feed concentration. Stability of the ELM is not crucial in HFC configurations because hollow fibers physically prevent the mixing of the feed phase and the extracting phase. Good extraction can be accomplished even without the use of surfactant. This suggests the possibility of eliminating the downstream demulsification process and the substantial reduction of the operating costs.

Acknowledgment

This project was partially funded by the Hazardous Substance Management Research Center of New Jersey and the New Jersey Department of Environmental Protection. LIX 84 was a courtesy of Henkel Corporation. Their contributions are greatly appreciated.

Notation

d = diameter of hollow-fiber membrane, cm; subscripts i, lm, and o represent inner, log-mean, and outer diameter, respectively
D = diffusivity, cm^2/s
H = hydrogen-ion concentration, mol/mL
k = mass-transfer coefficient, cm/s
L = total length of the fibers, cm
M = copper(II)-ion concentration, mol/mL
n = fiber number in an HFC
Pe = Peclet number, $d^2\cdot u/D\cdot L$
r = radius of hollow-fiber membrane, cm; subscripts i and o represent inner and outer radius, respectively
Re = Reynolds number, $d\cdot u/\nu$
Sc = Schmidt number, ν/D
Sh = Sherwood number, $k\cdot d/D$
u = flow velocity, cm/s
z = position along fiber axle, cm
ν = kinematic viscosity, cm^2/s
ρ = fluid density, g/mL
ΔP = pressure drop, $g/cm\cdot s^2$
Δz = a finite distance along fiber axle

Superscript and subscripts

$-$ = properties at $z-\Delta z$
i = internal phase
sm = membrane surface at the shell side
tm = membrane surface at the tube side

Literature Cited

Alexander, P. R., and R. W. Callahan, "Liquid-Liquid Extraction and Stripping of Gold with Microporous Hollow Fibers," *J. Memb. Sci.*, **35**, 57 (1987).

Bird, R. B., W. E. Stewart, and E. N. Lightfoot, *Transport Phenomena*, Chap. 2, Wiley, New York (1971).

Boyadzhiev, L., and E. Bezenshek, "Carrier Mediated Extraction: Application of Double Emulsion Technique for Mercury Removal from Waste Water," *J. Memb. Sci.*, **14**, 13 (1983).

Cahn, R. P., and N. N. Li, "Commercial Applications of Emulsion Liquid Membranes," ACS Meeting, Toronto, Canada (1988).

Draxler, J., W. Furst, and R. Marr, "Separation of Metal Species by Emulsion Liquid Membranes," *J. Memb. Sci.*, **38**, 281 (1988).

Fuller, E. J., and N. N. Li, "Extraction of Chromium and Zinc from Cooling Tower Blowdown by Liquid Membranes," *J. Memb. Sci.*, **18**, 251 (1984).

Goto, M., F. Kubota, T. Miyata, and F. Nakashio, "Separation of Yttrium in a Hollow Fiber Membrane," *J. Memb. Sci.*, **74**, 215 (1992).

Goto, M., T. Miyata, K. Uezu, T. Kajiyama, F. Nakashio, T. Haraguchi, K. Yamada, S. Ide, and C. Hatanaka, "Separation of Rare Earth Metals in a Hollow-Fiber Membrane Extractor Modified by Plasma-Graft Polymerization," *J. Memb. Sci.*, **96**, 299 (1994).

Gu, Z. M., D. Wasan, and N. N. Li, "Ligand-Accelerated Liquid Membrane Extraction of Metal Ions," *J. Memb. Sci.*, **26**, 129 (1986).

Ho, W., and N. N. Li, "Emulsion Liquid Membranes," *Membrane Handbook*, Chap. IX, W. Ho and K. Sirkar, eds., Van Nostrand Reinhold, New York (1992).

Hu, S. B., "Emulsion Liquid Membrane Extraction of Heavy Metals Using Hollow-Fiber Contactors," PhD Diss., Rutgers Univ., New Brunswick, NJ (1997).

Izatt, R. M., R. L. Bruening, W. Gen, M. H. Cho, and J. J. Christensen, "Separation of Bivalent Cadmium, Mercury, and Zinc in a Neutral Macrocycle-Mediated Emulsion Liquid Membrane System," *Anal. Chem.*, **59**, 2405 (1987).

Kitagawa, T., Y. Nishikawa, J. Frankenfeld, and N. N. Li, "Wastewater Treatment by Liquid Membrane Process," *Environ. Sci. Technol.*, **11**, 602 (1977).

Larson, K., B. Raghuraman, and J. Wiencek, "Electrical and Chemical Demulsification Techniques for Microemulsion Liquid Membranes," *J. Memb. Sci.*, **91**, 231 (1994).

Li, N. N., "Separation Hydrocarbon with Liquid Membranes," U.S. Patent No. 3,410,794 (1968).

Matsumoto, M., H. Shimauchi, K. Kondo, and F. Nakashio, "Kinetics of Copper Extraction with Kelex 100 Using a Hollow Fiber Membrane Extractor," *Solvent Extr. Ion Exch.*, **5**, 301 (1987).

Peters, R., and Y. Ku, "Batch Precipitation Studies for Heavy Metal Removal by Sulfide Precipitation," *Separation of Heavy Metals and Other Trace Contaminates*, AIChE Symp. Ser., Vol. 81, p. 9 (1985).

Prasad, R., and K. K. Sirkar, "Dispersion Free Solvent Extraction with Microporous Hollow Fiber Modules," *AIChE J.*, **34**, 177 (1988).

Press, W. H., S. A. Teukolsky, W. T. Vetterling, and B. P. Flannery, *Numerical Recipes in FORTRAN: The Art of Scientific Computing*, 2nd ed., Cambridge Univ. Press, New York (1992).

Raghuraman, B., and J. Wiencek, "Extraction with Emulsion Liquid Membranes in a Hollow-Fiber Contactor," *AIChE J.*, **39**, 1885 (1993).

Reid, R. C., J. M. Prausnitz, and T. K. Sherwood, *The Properties of Gases and Liquids*, 4th ed., McGraw-Hill, New York (1987).

Sato, Y., K. Kondo, and F. Nakashio, "A Novel Membrane Extractor Using Hollow Fibers for Separation and Enrichment of Metal," *J. Chem. Eng. Jpn.*, **23**, 23 (1990).

Sato, Y., K. Kondo, and F. Nakashio, "Extraction Kinetics of Molybdenum with 2-Ethylhexyl Phosphonic Acid Mono-2-Ethylhexyl Ester in Membrane Extractor Using a Hollow Fiber," *J. Chem. Eng. Jpn.*, **22**, 200 (1989a).

Sato, Y., K. Kondo, and F. Nakashio, "Extraction Kinetics of Zinc and 2-Ethylhexyl Phosphonic Acid Mono-2-Ethylhexyl Ester Using a Hollow-Fiber Membrane Extractor," *J. Chem. Eng. Jpn.*, **22**, 677 (1989b).

Schramm, L. L., "Petroleum Emulsion: Basic Principles," *Emulsions*, Chap. 1, L. L. Schramm, ed., The American Chemical Society, Washington, DC (1992).

Walsh, A. J., and H. G. Monbouquette, "Extraction of Cd^{2+} and Pb^{2+} from Dilute Aqueous Solution Using Metal-Sorbing Vesicles in a Hollow-Fiber Cartridge," *J. Memb. Sci.*, **84**, 107 (1993).

Weiss, S., and V. Grigoriev, "The Liquid Membrane Process for the Separation of Mercury from Waste Water," *J. Memb. Sci.*, **12**, 119 (1982).

Wiencek, J. M., and S. Qutubuddin, "Microemulsion Liquid Membranes. I. Application to Acetic Acid Removal from Water," *Sep. Sci. Technol.*, **27**, 1221 (1992).

Wickramasinghe, S. R., M. J. Semmens, and E. L. Cussler, "Better Hollow Fiber Contactors," *J. Memb. Sci.*, **69**, 235 (1992).

Yang, M., and E. L. Cussler, "Designing Hollow-Fiber Contactors," *AIChE J.*, **32**, 1910 (1986).

Yoshizuka, K., K. Kondo, and F. Nakashio, "Effect of Interfacial Reaction on Rates of Extraction and Stripping in Membrane Extractor Using a Hollow Fiber," *J. Chem. Eng. Jpn.*, **19**, 312 (1986).

Yun, C. H., R. Prasad, A. K. Guha, and K. K. Sirkar, "Hollow Fiber Solvent Extraction Removal of Toxic Heavy Metals from Aqueous Waste Streams," *Ind. Eng. Chem. Res.*, **32**, 1186 (1993).

Manuscript received June 9, 1997, and revision received Nov. 17, 1997.